Electronic structure and migrational properties of interstitial zinc in ZnSe

K. H. Chow and G. D. Watkins
Department of Physics, Lehigh University, Bethlehem, Pennsylvania 18015
(Received 30 April 1999)

We report optically detected electron paramagnetic resonance via photoluminescence in ZnSe after *in situ* 4.2 K irradiation with 2.5 MeV electrons. The isolated interstitial is identified in the T_d site surrounded by four zinc atoms, $(\mathrm{Zn}_i)^+_{\mathrm{Zn}}$, as well as in the T_d site surrounded by four Se atoms, $(\mathrm{Zn}_i)^+_{\mathrm{Se}}$. Analysis of the central ^{67}Zn and neighboring ^{77}Se atom hyperfine interactions for the two sites, plus other considerations, allows estimates of their second donor levels to be at $\sim$1.6 and $\sim$1.0 eV below the conduction band, respectively. Migration of the interstitial under optical excitation at 1.5–25 K is detected by monitoring its cyclic conversion between the two configurations, as well as by interconversion between various close zinc-interstitial–zinc-vacancy Frenkel pairs. The dependence of the process on temperature, excitation wavelength and intensity, and sample history is described, and a possible model for the mechanism is proposed. [S0163-1829(99)16235-0]

I. INTRODUCTION

ZnSe, which has been irradiated with 2.5 MeV electrons *in situ* at 4.2 K, is a fascinating system. The effect of such an irradiation is to produce a large number of intrinsic lattice defects, which are frozen into the lattice at these low temperatures. First observed directly by electron paramagnetic resonance (EPR),[1] and later primarily through the use of optically detected EPR (ODEPR) via photoluminescence (PL),[2,3] these centers have been identified and characterized as being zinc-interstitial–zinc-vacancy Frenkel pairs with varying intramolecular separations. Most of the observed PL bands arise from radiative electron-hole recombination in the 700–1100 nm region involving the zinc-interstitial donor and its partner vacancy acceptor:

$$\mathrm{Zn}_i^+ + V_{\mathrm{Zn}}^- \rightarrow \mathrm{Zn}_i^{2+} + V_{\mathrm{Zn}}^{2-} + h\nu, \tag{1}$$

where the Zn_i^+ and V_{Zn}^- centers are paramagnetic. The above reaction has been found to be appropriate for four very close ODEPR pairs labeled $A-D$ (strongly exchange-coupled into $S=1$ emitting systems), many at intermediate distances, labeled X_1–X_{20} (less strongly exchange-coupled donor-acceptor $S=\frac{1}{2}$ pairs), to pairs which are so ''distant'' that the exchange interaction is approximately zero. For all these centers, the evidence indicates that the zinc interstitial is located at the T_d site with four nearest-neighbor Se atoms, which we denote $(\mathrm{Zn}_i)^+_{\mathrm{Se}}$.

In addition, zinc interstitials can also be observed which are so far separated from their companion vacancies that they are for all practical purposes *isolated*. In contrast to the pairs above, these centers are observed via a competing spin-dependent recombination process,

$$(\mathrm{Zn}_i)^+ + \mathcal{D}^0 \rightarrow (\mathrm{Zn}_i)^0 + \mathcal{D}^+, \tag{2}$$

which produces *negative* $(\mathrm{Zn}_i)^+$ ODEPR signals in radiative distant shallow $\mathcal{D}^0$ donor to deep acceptor $\mathcal{A}^0$ recombination at $\approx$625 nm,

$$\mathcal{A}^0 + \mathcal{D}^0 \rightarrow \mathcal{A}^- + \mathcal{D}^+ + h\nu. \tag{3}$$

Here, either of two deep acceptors $\mathcal{A}$ can be involved—a very close Frenkel pair, labeled V^I, or, after it anneals out at an early stage ($\sim$60 K), the vacancy-donor ''self-activated'' center originally present in the sample. From the detection of weak resolved hyperfine interactions with the central ^{67}Zn ($I=5/2$, 4.1% abundant) atom, and ^{77}Se ($I=1/2$, 7.6% abundant) atoms in the first- and third-neighbor shells, it has been unambiguously demonstrated that the dominant negative signal arises from $(\mathrm{Zn}_i)^+_{\mathrm{Se}}$, and important details of its electronic structure have been deduced.[2,4] A second weaker negative signal was also observed. Its identification was not as clear in this early work, and hence it was labeled as *X*. However, evidence was presented to suggest a tentative assignment as $(\mathrm{Zn}_i)^+_{\mathrm{Zn}}$, where the Zn_i^+ is now located at the other T_d site surrounded by four Zn atoms. In the present paper, we will unambiguously confirm this identification and deduce important details concerning its electronic structure. In Fig. 1, we summarize in an energy-level dia-

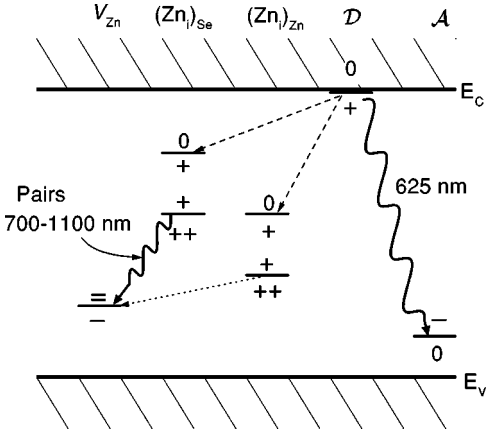

FIG. 1. Schematic of the energy-level positions within the band gap of ZnSe for the isolated vacancy V_{Zn}, the isolated zinc interstitials $(\mathrm{Zn}_i)_{\mathrm{Se}}$ and $(\mathrm{Zn}_i)_{\mathrm{Zn}}$, the shallow donor $\mathcal{D}$, and the deep acceptor $\mathcal{A}$. The solid wavy arrows indicate observed radiative transitions, the dashed arrows competitive processes, and the dotted arrow the as-yet unobserved transitions for $(\mathrm{Zn}_i)_{\mathrm{Zn}}$-related Frenkel pairs.

gram the relevant transitions of Eqs. (1)–(3).

Recently, in a preliminary report, we cited evidence that the interstitial zinc atom could be made to migrate under optical excitation at cryogenic temperatures.[5] Such a phenomenon falls under the general category of *recombination enhanced migration* (REM),[6] where a large concentration of injected electrons and holes or direct optical excitation leads to motion of a relevant defect. Mechanisms suggested for REM include a charge-state-dependent energy barrier for diffusion, or energy release processes where the excitation energy supplied to a defect (e.g., from electron and/or hole capture, or direct optical excitation) is nonradiatively converted into kinetic energy that helps it to surmount its migration barrier in either its ground or excited state.[6–8] In addition to being of fundamental scientific interest, the observation of efficient recombination-enhanced motion for interstitial zinc clearly has technological ramifications regarding degradation of ZnSe-based laser devices.

In the present paper we will describe the experiments which have led to this conclusion, exploring in detail the various thermally and optically induced kinetics for the interstitial migration and its consequent effects on the Frenkel pairs. Critical to the interpretation will be the identification and new electronic-structure information concerning the $(\mathrm{Zn}_i)^+_{\mathrm{Zn}}$ interstitial site. We begin the paper with a brief outline of the experimental aspects (Sec. II). Then, in Sec. III we describe, in various subsections, the experimental results, including the effect of alternate electronic excitation and thermal annealing on the individual pairs, the identification and electronic-structure determination of $(\mathrm{Zn}_i)^+_{\mathrm{Zn}}$, and the kinetics of the back and forth diffusional jump between the two interstitial sites. In Sec. IV, we discuss the various results and their interpretation, and in the final section, we provide a brief summary of what has been learned.

II. EXPERIMENTAL PROCEDURE

The experimental setup used to obtain the data described in this paper is identical to that of earlier ODEPR work,[2] which should be referred to for details. Briefly, the experiments were performed at 20 GHz in an EPR spectrometer capable of *in situ* 4.2 K electron irradiation with 2.5 MeV electrons from a Van de Graaff accelerator. Subsequent ODEPR experiments were accomplished by inserting into the TE_{011} microwave cavity a capillary tube which served as a light pipe to extract the photoluminescence, and through which is threaded an optical fiber which allowed for the sample (which is located a few millimeters below the light pipe) to be photoexcited. The sample was immersed in pumped liquid helium ($\approx$1.5 K) during such experiments. The excitation was supplied primarily by the 458 nm or 476.5 line of an argon ion laser and the luminescence detected by either a silicon (EG&G 250 UV) or cooled germanium (North Coast EO-817S) diode detector. The microwave power was on-off modulated at various audiofrequencies, and synchronous changes in the luminescence were detected via lock-in detection. Different choices of experimental conditions such as magnetic field orientation, modulation frequency of microwaves, and wavelength of excitation light were used to optimize the detection of the various centers. More details can be found in Refs. 2 and 3.

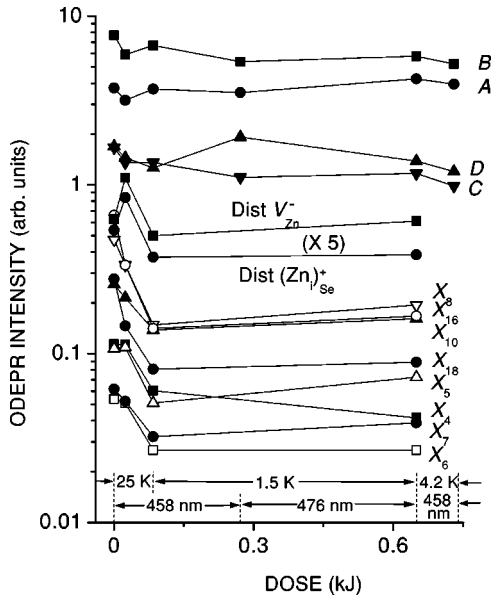

FIG. 2. ODEPR signal intensities of various Frenkel pairs after two 25 K anneals with 458 nm (22 mW) excitation, and subsequent 458 nm (22 mW) and 476.5 nm (47 mW) excitation at 1.5 K and 4.2 K, as indicated.

The samples studied were single crystals cut from boules grown by vapor transport in a sealed quartz ampoule, and supplied either by the G. E. Research and Development Center or Phillips Laboratory. The samples will be referred to as GE or PhL, respectively. Unless otherwise stated, the experiments were performed on the as-grown high-resistivity *n*-type crystals. In one case, to be specifically noted, a zinc-fired low-resistivity *n*-type sample was also studied.

III. EXPERIMENTAL RESULTS

A. Frenkel pair conversions

After electron irradiation of a high-resistivity as-grown sample at 4.2 K, the complete set of Frenkel pairs previously reported ($A-D$ very close $S=1$ exchange-coupled pairs, $X_1 \rightarrow X_{20}$, exchange-coupled $S=\frac{1}{2}$ pairs of progressively increasing separations, and distant pairs for which the exchange is undetectable)[2] are observed. Examples of the ODEPR spectra of these centers are shown in Figs. 6 and 7 of Ref. 2. Under the normal low power laser excitation ($\lesssim$3 mW) for the PLODEPR studies at 1.5 K, the intensity of each is quite stable, showing little evidence of change over many days of study. However, optical excitation at $\sim$25 K produces significant changes, as illustrated in Fig. 2 for representative members of the pairs. Little change is seen for the $A-D$ very close pairs, substantial decreases are observed for the intermediate pairs, while the well separated coupled pairs first increase and then decrease. The intensity changes of the individual intermediate pairs also differ, decreasing by a factor of $\sim 2\times$ to as much as $5\times$. Shown, in addition, is that continuing with prolonged excitation at 1.5 K also produces further changes, albeit more slowly. From this, it is clear that one of the two constituents—the zinc vacancy or interstitial—must be migrating at these temperatures, and the general pattern strongly suggests that the net flow is one of separation.

Another interesting observation results when the initial electron irradiation is performed with the beam aligned along a crystal [111] or $[\overline{1}\overline{1}\overline{1}]$ direction. As demonstrated in the previous studies,[2] this produces preferential alignment of the various pairs with respect to the beam direction, a result of the primary displacement process. This initial alignment, which can be monitored directly from the ODEPR intensities of the differently oriented pairs, is observed to exist for all of the prominent defect pairs, up to even the most distant pairs with no resolvable exchange splittings. (The Coulomb interaction is still important for the most distant pairs; hence, the hole on the vacancy preferentially locates on its Se neighbor that is farthest removed from the positively charged interstitial. The vacancy anisotropy therefore reveals the direction of its companion interstitial.)

During the optically induced rearrangements and separation that are occurring, no significant change in the degree of alignment is observed for any of the pairs. This remarkable result reveals that in the diffusion process, the direction vector separating the pairs does not significantly wander between the spatial quadrants around each of the $\langle 111\rangle$ directions, the motion therefore being weighted in the direction of separation.

Now let us concentrate on conversion between the very close pairs. We first thermally anneal to 150 K in the dark, which, as has been previously demonstrated,[2] preferentially removes the *A* and *C* spectra, leaving *B* and *D* and all of the other pairs essentially unchanged. Next we illuminate the sample at 1.5 K with 458 nm light, and monitor the ODEPR spectra. As shown in Fig. 1 of our previous publication,[5] spectrum *A* progressively reemerges with a corresponding 1:1 decrease in *B*. This result suggests strongly that *A* is being regenerated by conversion from *B*. The conversion is not complete, saturating in those results at the fixed ratio $A/B \sim 0.7$, revealing that the conversion process goes in both directions, i.e., $B \leftrightarrows A$. Here we were apparently monitoring directly the one-jump process between the two configurations, which occurs even at 1.5 K. The time constant for the conversion at ~ 25 mW excitation was measured to be ~ 330 min.

The sample used in that study was a PhL one that had been electron-irradiated and subsequently annealed to room temperature several times before electron-irradiating it again. In Fig. 3 of the present paper, we present the results of a similar study for a GE sample, which had a significantly lower prior accumulated dose. For this experiment, the individual pairs were initially aligned as a result of electron irradiation along the crystal $[\overline{1}\overline{1}\overline{1}]$ direction. Shown in the figure for both *A* and *B* are the measured intensities of the defects for each which are aligned along the beam direction as well as those along a different $\langle 111\rangle$ direction. The additional important information contained here is the observation that *A* reemerges with the same sense of alignment as before the anneal. Subtracting the initial concentration of *A*, the alignment in the freshly generated *A* signals is within accuracy equal to that observed in *B*, confirming again the 1:1 correspondence. We note further in the figure that for this sample, the $B \rightarrow A$ conversion rate is approximately the same as for the PhL sample, ~ 360 min, but the A/B saturation ratio appears smaller, ~ 0.25.

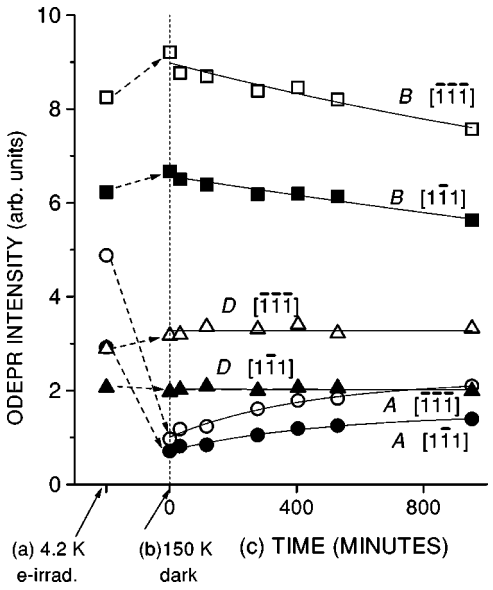

FIG. 3. The ODEPR intensities of close pairs *A*, *B*, and *D*, which are aligned along the $[\overline{1}\overline{1}\overline{1}]$ or $[1\overline{1}\overline{1}]$ directions of a crystal (a) after an electron irradiation along $[\overline{1}\overline{1}\overline{1}]$; (b) after a subsequent anneal in the dark to 150 K; and (c) vs subsequent optical excitation with 458 nm (27 mW power) at 1.5 K.

In the *n*-type Zn-fired sample, strong $A-D$ close pair signals were also produced by electron irradiation. However, in that sample, it was found that *A* and *B* anneal together at 150 K. It was therefore not possible to study the $B \leftrightarrows A$ conversion for it. In addition, the more distant pair and isolated interstitial signals were very weak in this sample and therefore no systematic attempts to study their evolution versus optical excitation, as in Fig. 2, were attempted. We will discuss more experiments on this sample in Sec. III E 3.

B. Identification of $(Zn_i)_{Zn}$

In Fig. 4(a), we show the isolated interstitial $(Zn_i)^+_{Se}$ PLODEPR signal. As discussed in the Introduction, its negative signal arises from a shallow donor to Zn_i^+ recombination, Eq. (2), which competes with the 625 nm shallow donor to deep acceptor recombination luminescence being monitored, Eq. (3). In the earlier studies,[2] the hyperfine structure of ^{77}Se ($I=1/2$, 7.6% abundant) could be resolved for the four nearest neighbors, and partially resolved for the third-nearest-neighbor shell, confirming that Zn_i^+ occupies the interstitial site surrounded by four Se atoms. The presence of the on-center Zn atom was confirmed by the detection of weak isotropic satellites of its central isotropic ODEPR line due to hyperfine interaction with the ^{67}Zn ($I=\frac{5}{2}$, 4.1% abundant) nuclear isotope of the central atom. This required multiple signal averaging, since the intensity of each ^{67}Zn satellite is only $\sim 0.7\%$ of the central line.

In addition, a second isotropic but weaker negative resonance with a slightly larger *g* value is also observed. This signal was labeled *X* in the earlier studies. Shown in Fig. 4(b) is the interesting result of 458 nm illumination at 25 K, followed by a rapid cooldown to 4.2 K. The *X* signal has grown significantly and is now the dominant one, the $(Zn_i)^+_{Se}$ signal having decreased in proportion. This 1:1 conversion provides

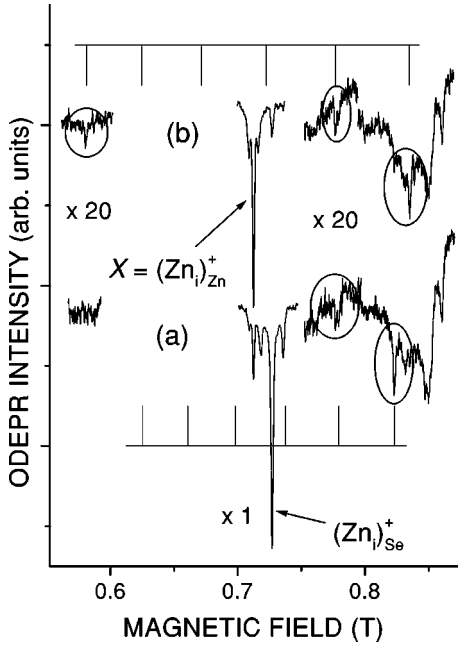

FIG. 4. The ODEPR spectra of the isolated zinc interstitials $(Zn_i)^+_{Se}$ and $(Zn_i)^+_{Zn}$ with $\mathbf{B}\|\langle 100\rangle$. (a) After anneal at 25 K in the dark, the $(Zn_i)^+_{Se}$ signal is dominant. (b) After 458 nm illumination at 25 K, the $(Zn_i)^+_{Zn}$ signal dominates. In both (a) and (b), observed satellites arising from hyperfine interaction with the central Zn_i ion are circled. Also shown for comparison are the theoretically predicted positions for all of the satellites, calculated using the relevant ^{67}Zn hyperfine parameters listed in Table. I.

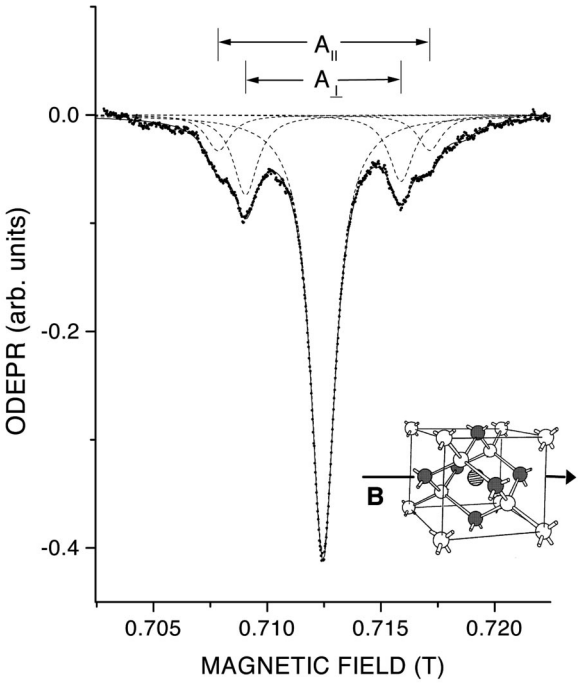

FIG. 5. The central $(Zn_i)^+_{Zn}$ ODEPR signal with $\mathbf{B}\|\langle 100\rangle$. The shoulders are due to the Se shell at second-nearest-neighbor positions, as indicated by the darkened atoms in the inset. The solid line is a fit of the data assuming identical Lorentzian line shapes for the central and satellite lines. The dashed curves show the contributions of each individual line.

a strong clue that X also arises from Zn_i, but in a different lattice configuration. Taking advantage of this newly discovered ability to increase its intensity, it becomes possible now to perform the same critical hyperfine interaction measurements on it. During the many required signal averaged runs at 1.5 K, it was found that a slow reverse conversion back to $(Zn_i)^+_{Se}$ was occurring. It was necessary, therefore, to regenerate X by the 25 K optical excitation process periodically during the runs. In a subsequent section we will study the kinetics of these changes, but we concentrate here first on the identification of X.

The results of the many signal averaged runs are shown in Fig. 4 , where the spectra are shown under higher gain in the regions free of overlap with unrelated spectra when either one or the other of the two interstitial-related spectra is dominant. That X does indeed arise from interstitial zinc is confirmed by the observation of three of the six expected ^{67}Zn hyperfine lines, which can be seen in the figure to correlate in intensity with that of the central line, as it changes between (a) and (b). Shown also in (a) are two of the corresponding satellites for the $(Zn_i)^+_{Se}$ signal, which now emerge when the $(Zn_i)^+_{Se}$ central line is strong. Shown in Fig. 5, on an expanded magnetic field scale, is additional satellite structure on the shoulders of the X central line.

The positions of the central line and its satellites can be fit by the $S=\frac{1}{2}$ spin Hamiltonian

$$\mathcal{H}=g\mu_B\mathbf{B}\cdot\mathbf{S}+\sum_j \mathbf{I}_j\cdot\mathbf{A}_j\cdot\mathbf{S}, \tag{4}$$

where the first term describes the isotropic electronic Zeeman interaction in a magnetic field $\mathbf{B}$ and the second term describes the hyperfine interactions with the central ^{67}Zn atom nucleus and neighboring ^{77}Se nuclei. For the neighboring ^{77}Se atoms, the hyperfine interaction is found to be closely axially symmetric with

$$A_\parallel = a+2b,$$
$$A_\perp = a-b, \tag{5}$$

where a is the isotropic part, b is the anisotropic part, and the axis reflects the direction from the site to the central interstitial zinc atom. The relevant parameters are summarized in Table I, which also includes for comparison the previous experimental data on $(Zn_i)^+_{Se}$.

The hyperfine interaction with the central ^{67}Zn nucleus produces six $(2I+1)$ satellites, whose positions, determined from the three detected, are indicated in Fig. 4(b). The interaction is isotropic, consistent with the T_d symmetry of a $(Zn_i)_{Zn}$ site. The resolved structure on the shoulders of the central line, Fig. 5 , matches well with the intensities predicted for a total of six ^{77}Se nuclei. These are identified to be due to the six Se second-nearest-neighbor atoms which are equidistant in each of the six $\langle 100\rangle$ directions from the central $(Zn_i)^+_{Zn}$ ion. Consistent with this, angular dependence studies reveal that the interaction for each has axial symmetry about its corresponding $\langle 100\rangle$ axis.[9] The data in Fig. 5, which were obtained with $\mathbf{B}$ parallel to a $\langle 100\rangle$ axis, should hence be made up of contributions due to two equivalent nuclei with effective hyperfine interaction $A_\parallel$ and four

TABLE I. Experimental spin Hamiltonian parameters for isolated Zn_i^+ at the two interstitial T_d sites in ZnSe, compared to estimates from theory. The numbers in parentheses represent the error estimates in the last digit of each entry. The hyperfine parameters are given in MHz.

	$(Zn_i)^+_{Se}$ Expt [a]	Theory		$(Zn_i)^+_{Zn}$ Expt	Theory
g	1.9964(4)			2.0064(5)	
$a(^{67}Zn)$	1088(15)	1078,[b] 1067 [c]	$a(^{67}Zn)$	1425(8)	1252,[b] 1739 [c]
$a(^{77}Se)_{1NN}$	481(3)	736,[b] 355 [c]			
$b(^{77}Se)_{1NN}$	17(3)	11,[b] 17 [c]			
			$a(^{77}Se)_{2NN}$	215(3)	354,[b] 227 [c]
			$b(^{77}Se)_{2NN}$	23(2)	20[c]
$a(^{77}Se)_{3NN}$	37(3)	55[b]			

[a]Ref. 2.
[b]Ref. 19.
[c]Ref. 20.

equivalent nuclei with effective interaction $A_\perp$. This is indeed confirmed by the relative intensity of the shoulders compared to the central line, where the indicated match in the figure corresponds to two and four equivalent nuclei being responsible for $A_\parallel$ and $A_\perp$, respectively. In contrast to $(Zn_i)^+_{Se}$, no additional structure is seen on the central line itself, which is narrower, indicating relatively weaker hyperfine interaction at the fourth, and more distant neighbor ^{77}Se shells.

These results demonstrate unambiguously therefore that, as tentatively suggested in previous work,[2,4] the so-called X center is indeed $(Zn_i)^+_{Zn}$ located at the T_d site surrounded by four nearest-neighbor Zn atoms.

C. The electronic structure of $(Zn_i)^+_{Zn}$

The central $^{67}(Zn_i)^+_{Zn}$ hyperfine interaction (1425 MHz) is 31% greater than that for $^{67}(Zn_i)^+_{Se}$ (1088 MHz), indicating that the unpaired electron is more highly localized on it, and that its corresponding second donor level $(+/++)$ is therefore deeper in the gap. To pursue this point further, we proceed, as was previously done for $(Zn_i)^+_{Se}$, to treat the electron as bound in a spherically symmetric envelope function which is orthogonalized to the ion cores of the atoms. The advantage of such an approach is that it can provide an approximate guide as to the binding energy of the electron to the interstitial and hence the level position in the gap.

As discussed in more detail in Ref. 2, orthogonalizing an envelope function $\Phi(\mathbf{r})$ to the ion cores of the lattice atoms gives for the electron wave function

$$\psi(r)=N\left\{\Phi(\mathbf{r})-\sum_{j,\alpha}\phi_j^\alpha\langle\phi_j^\alpha|\Phi(\mathbf{r})\rangle\right\}, \tag{6}$$

where ϕ_j^α denotes the αth core orbital of atom j and N is a normalization factor. Assuming the envelope function to be slowly varying over the extent of each of the core orbitals leads to

$$|\psi(r_j)|^2\approx G_j N^2|\Phi(r_j)|^2, \tag{7}$$

where

$$G_j=\left|1-\sum_\alpha \phi_j^\alpha(0)\int\phi_j^\alpha dV\right|^2. \tag{8}$$

We use the experimental isotropic part of the hyperfine constants a_j to estimate $|\psi(r_j)|^2$ using

$$a_j=\frac{(A_\parallel)_j+2(A_\perp)_j}{3}=\frac{16\pi}{3}\left(\frac{\mu_j}{I_j}\right)\mu_B|\psi(r_j)|^2, \tag{9}$$

where μ_j and I_j are the nuclear magnetic moment and spin of the jth nucleus while μ_B is the Bohr magneton. G_j can be calculated using self-consistent Hartree-Fock functions for the free Zn^{2+} and Se^0 ions,[10] which can be used in conjunction with Eq. (7) to determine $|\Phi(r_j)|$. The results for the central zinc atom and the next neighbor Se shell for $(Zn_i)^+_{Zn}$

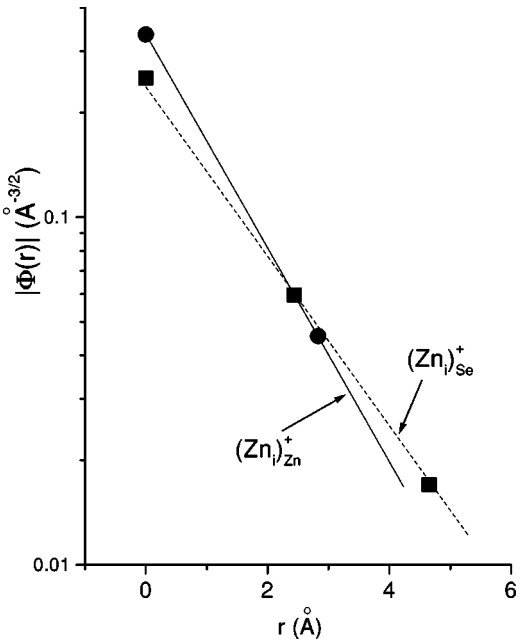

FIG. 6. The amplitude of the $\Phi(r)$ envelope wave function for $(Zn_i)^+_{Zn}$ (closed circles) deduced from hyperfine interactions and its corresponding fit (solid line) as described in the text. The $(Zn_i)^+_{Se}$ results from Ref. 2 are reproduced here for comparison (closed squares and dashed line).

are plotted in Fig. 6, and are compared to the values determined for $(Zn_i)^+_{Se}$. For each, the straight line corresponds to a simple exponential dropoff, which, in turn, leads to a straightforward determination of N [0.81 for $(Zn_i)^+_{Zn}$, 0.93 for $(Zn_i)^+_{Se}$], which has been used in the evaluation of $\Phi(\mathbf{r}_j)$.

As in the previous publication, we assume the one-electron envelope wave function for the unpaired electron of Zn_i^+ to be similar to that of a $Z=2$ hydrogenic atom in a uniform dielectric and, furthermore, that, for such a tightly bound state, the electron mass should be close to the free electronic value m. The solution is hence

$$\Phi_{He^+}(r)=\frac{1}{(\pi a_0^3)^{1/2}}\exp(-r/a_0), \tag{10}$$

with a binding energy

$$E=\frac{2me^4}{\varepsilon^2\hbar^2} \tag{11}$$

and Bohr radius

$$a_0=\frac{\varepsilon\hbar^2}{2me^2}=\frac{\hbar}{\sqrt{2mE}}. \tag{12}$$

The slope of the straight line for $(Zn_i)^+_{Zn}$ gives $a_0=1.44$ Å, corresponding to an effective dielectric constant $\varepsilon=5.4$ and a binding energy of 1.8 eV. Note that as expected for a tightly bound state, ε is close to the high-frequency value $\epsilon_\infty\sim 6$. This result, when compared with that obtained for $(Zn_i)^+_{Se}$ by the same method of 1.2 eV, suggests that the second donor level $(+/++)$ for $(Zn_i)_{Zn}$ could be as much as ~ 0.6 eV deeper than that for $(Zn_i)_{Se}$. This has been incorporated in Fig. 1. An alternative estimate of $E_c-0.9$ eV, suggested to perhaps be more accurate, was also made for the $(Zn_i)^+_{Se}$ level in the earlier work by considering the photoluminescence energy of one of the Frenkel pairs whose separation was believed to be established.[2] Assuming a proportional overestimate here for $(Zn_i)^+_{Zn}$ suggests its level to be ~ 0.4–0.5 eV lower, i.e., at $\sim E_c-1.4$ eV.

D. $(Zn_i)_{Se}\leftrightarrows(Zn_i)_{Zn}$ conversion

In Fig. 7, we summarize the result of sequential annealing and illumination steps on the intensity of the two Zn_i^+ signals. For this particular sample (GE), annealing in the dark to 25 K completely removes the $(Zn_i)^+_{Zn}$ signal, with a corresponding increase in the $(Zn_i)^+_{Se}$ signal. Subsequent 458 nm illumination at 25 K with a rapid cooldown regenerates it, so that it is now the dominant one, with a corresponding decrease in the $(Zn_i)^+_{Se}$ signal, as also shown in Fig. 4, and discussed in the previous sections. Upon subsequent 458 nm illumination at 1.5 K, slow, partial, return conversion is observed, demonstrating that optically induced conversion occurs in both directions, i.e., $(Zn_i)^+_{Zn}\rightleftarrows(Zn_i)^+_{Se}$, even at this low temperature. By repeating each of these injection and annealing processes, the interstitial can be controllably cycled back and forth many times between the two configurations. These results unambiguously demonstrate that the interstitial zinc is mobile under these excitation conditions,

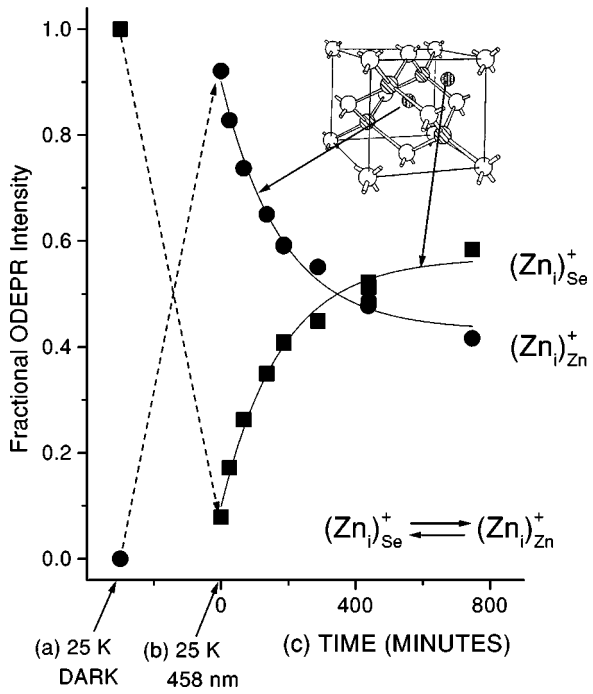

FIG. 7. The two isolated $(Zn_i)^+$ ODEPR signal intensities after (a) 25 K anneal in the dark, (b) subsequent 458 nm excitation at 25 K with a rapid cooldown to 4.2 K, and (c) vs subsequent accumulated dose of 458 nm (power 27 mW) light at 1.5 K.

conversion between the two sites and back constituting a *single diffusion jump*, each site representing an intermediate position from which a return jump carries the atom to four possible choices of the other.

Keeping in mind that the intensities of both $(Zn_i)^+_{Se}$ and $(Zn_i)^+_{Zn}$ remain unchanged in the dark at 4.2 K and below, these observations demonstrate that both the $(Zn_i)_{Se}\rightarrow(Zn_i)_{Zn}$ and $(Zn_i)_{Zn}\rightarrow(Zn_i)_{Se}$ processes are being produced by the optical excitation. The two rates are roughly comparable at 1.5 K. However, their temperature dependencies must be different, the $(Zn_i)_{Se}\rightarrow(Zn_i)_{Zn}$ conversion becoming dominant at higher temperature. A preliminary study of the temperature dependence of the $(Zn_i)_{Zn}\rightleftarrows(Zn_i)_{Se}$ rate reveals no significant change between 1.5 K and 4.2 K, but an increase of $>10^3$ already by 10 K. (The time constant measured with 250 μW 458 nm excitation at 10 K is ~ 1.5 min.) For the 25 K optical generation of $(Zn_i)^+_{Zn}$, it is therefore sufficient to illuminate with a modest power for only a few seconds, and quench by refilling with liquid helium with the light on.

In Fig. 8, we show the rather broad wavelength dependence of the $(Zn_i)^+_{Zn}\rightleftarrows(Zn_i)^+_{Se}$ conversion rate at 1.5 K, obtained at a few other convenient argon ion laser wavelengths. In Fig. 9, we show the dependence of the rate at 1.5 K versus 458 nm optical excitation power, measured on a freshly irradiated as-grown GE crystal. The rate dependence is linear up to ~ 2.5 mW but clearly saturates at higher power levels. In the majority of our experiments, a power level $\leqslant 2.5$ mW was used for monitoring the spectra and ~ 27 mW for the conversion process studies.

The data of Fig. 7 were obtained for a GE as-grown sample after one anneal to room temperature and second electron irradiation. In all as-grown samples studied (i.e.,

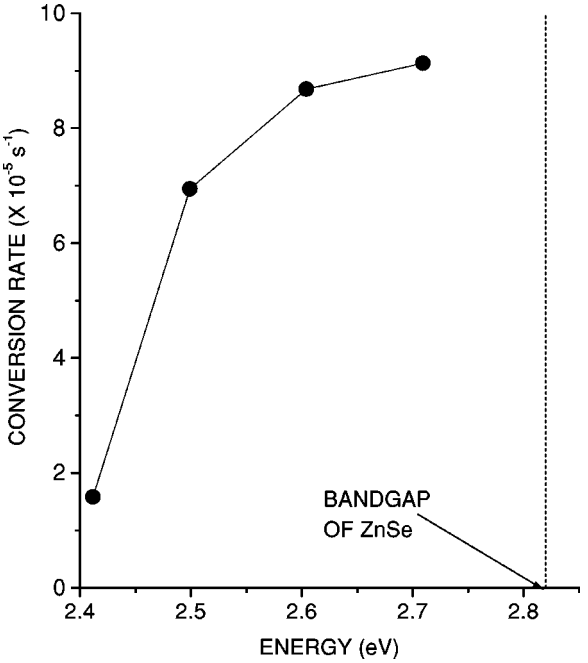

FIG. 8. The $(Zn_i)^+_{Zn} \rightleftarrows (Zn_i)^+_{Se}$ conversion rate at 1.5 K vs energy of the exciting light. The band gap (2.82 eV) of ZnSe is also indicated in the figure.

PhL or GE), the same conversion processes could be made to occur, but with some differences. It was found, for example, that after several room-temperature anneals and reirradiations on a single sample, only partial loss of $(Zn_i)^+_{Zn}$ was found to occur in the dark at 25 K. Complete loss required anneal to $\sim$150 K. In addition, the optically induced $(Zn_i)^+_{Zn} \rightleftarrows (Zn_i)^+_{Se}$ conversion rate at 1.5 K was reduced by as much as a factor $\sim$10. Similarly, in another sample with significantly less accumulated prior electron irradiation dose, the 1.5 K cyclic conversion rate decreased by a factor of

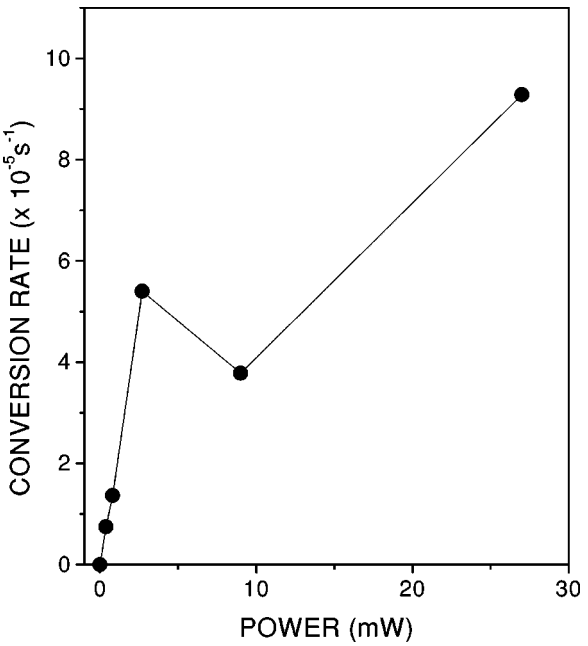

FIG. 9. The power dependence of the $(Zn_i)^+_{Zn} \rightleftarrows (Zn_i)^+_{Se}$ conversion rate under 458 nm excitation at 1.5 K.

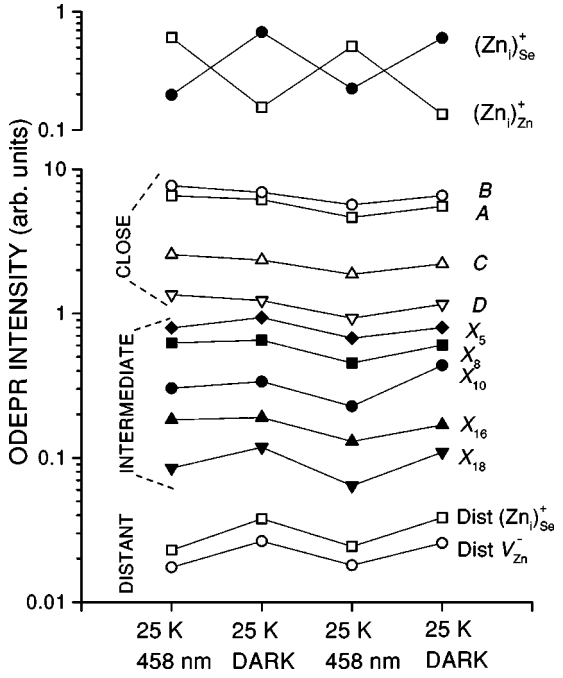

FIG. 10. Relative changes in the ODEPR amplitudes of various $(Zn_i)^+_{Se}$-related Frenkel pairs compared to those for $(Zn_i)^+_{Se}$ and $(Zn_i)^+_{Zn}$ as the sample is alternately optically excited or annealed in the dark at 25 K. In the lower panel, for purposes of clarity, the intensities of some of the Frenkel pairs have been shifted vertically.

$\sim$2.5 after prolonged optical excitation and subsequent annealing to $\gtrsim$220 K to remove almost all Frenkel pair spectra, while still retaining the isolated Zn_i^+ spectra.

E. Additional experiments

1. $(Zn_i)^+_{Zn}$-related Frenkel pairs

In light of our observation that isolated $(Zn_i)^+_{Zn}$ exists, it is relevant to inquire why the ODEPR is not seen for close and intermediate Frenkel pairs where the zinc interstitial is located at the T_d(Zn) site. The Frenkel pairs which have thus far been observed have all been previously identified as $(Zn_i)^+_{Se}$-related and show luminescence in the visible and near infrared. As can be seen in Fig. 1, a significantly deeper level position for the $(+/++)$ level implies that even if the $(Zn_i)^+_{Zn}$-related Frenkel pairs also exhibit radiative luminescence, their PL bands would appear at correspondingly lower ($\sim$0.4–0.6 eV) energies, placing them further into the infrared, perhaps out of the range of our Ge detector ($>$0.66 eV). We have therefore initiated an attempt to extend the measured range with an InAs detector, being limited in that case by light absorption in the long quartz lightpipe ($>$0.5 eV). The noise was found to be significantly greater, and as yet our experiments have revealed no new signals.

However, there is indirect evidence that such centers do indeed exist, as indicated in Fig. 10, which shows the ODEPR amplitudes of various $(Zn_i)^+_{Se}$-related Frenkel pairs after the sample is alternately optically excited or annealed in the dark at 25 K. A small but significant correlated decrease or increase is observed in the intensities of these pairs, particularly for the more distant ones, as expected if ''invisible'' $(Zn_i)^+_{Zn}$-related Frenkel pairs do indeed exist, and

whose fractional concentration partially reflects also the conversions for the isolated interstitials. The fact that the changes appear more evident for the more distant pairs suggests that the perturbation of the nearby vacancy serves to favor the $(Zn_i)^+_{Se}$ site.

2. Luminescence associated with isolated $(Zn_i)^+$

The isolated $(Zn_i)^+_{Se}$ and $(Zn_i)^+_{Zn}$ donors are detected as negative signals most strongly in the shallow donor to deep acceptor visible luminescence, Eq. (3), due to a competitive spin-dependent electron transfer process to them, Eq. (2). They can also be seen as weaker negative signals in the close and more distant pair luminescence, with which the process also competes, as well as in weak PL from other unrelated sources present throughout the full spectral region of the detectors. However, we have found no spectral region available to our silicon and cooled germanium detectors ($\geqslant 0.7$ eV), where they convert to positive signals, as would occur if the electron transfer process to them were radiative and dominant in the spectral region being detected. (To increase the sensitivity in one set of runs, we first removed most of the close and distant coupled pair ODEPR spectra by prolonged optical excitation at ~ 25 K, while still retaining the truly isolated interstitial negative signals. Again, no positive interstitial signals were detected.)

In this study, we also carefully investigated the luminescence system with a zero-phonon line at 0.907 eV, which was previously reported and suggested possibly to be related to interstitial zinc.[2] We were able to detect the signal clearly, which conveniently just misses the strong water absorption band in the quartz rod, but again, only negative $(Zn_i)^+$ signals were observed in it. In addition, subsequent annealing of the sample to $\gtrsim 200$ K in the dark removed the 0.907 eV luminescence completely, but the $(Zn_i)^+$ signals remained. We can conclude, therefore, that the 0.907 eV luminescence is not related to isolated interstitial zinc. It remains an interesting system, however, and is clearly intrinsic-defect related, being observed only after low-temperature electron irradiation and subsequent anneal to ≈ 100 K. Furthermore, since its annealing properties and presence/absence do not seem to be correlated with any of the defects involving the zinc sublattice, we are left with the possibility that the ZPL is due to a defect on the Se sublattice.

3. n-type samples

Recent state-of-the-art local-density calculations have been reported for interstitial zinc in each of its two T_d sites.[11] The authors find the total energy for $(Zn_i)^+$ to be identical in the two sites within the stated accuracy of the calculations. Our annealing results in the dark suggest that the $(Zn_i)^+_{Se}$ configuration is actually the thermodynamically stable one, but our ease in converting between the two configurations is clearly consistent with their relative stabilities being close. The authors also predicted that the electron binding energy for the neutral interstitial is ~ 0.4 eV greater for $(Zn_i)_{Zn}$ than for $(Zn_i)_{Se}$.[12] If correct, there is the possibility that it could become the thermodynamically stable configuration in *n*-type material.

It was to check this possibility that a Zn-fired *n*-type sample was also studied. The sample was verified to be low resistivity *n*-type before and after the irradiation by monitoring the shallow donor resonance directly by conventional EPR. Unfortunately, as mentioned in Sec. III A, even though the $A-D$ very close pair signals were strong, the intermediate and more distant pairs were considerably weaker than in the as-grown samples, and the isolated interstitial zinc signals were weaker still. Apparently, it is either more difficult to produce the more separated pairs, or they are less efficient in their corresponding recombination processes, in the *n*-type material.

Both $(Zn_i)^+_{Se}$ and $(Zn_i)^+_{Zn}$ could be observed very weakly with roughly equal intensities after integration with multiple scans. However, except for the observation that annealing in the dark at 50 K did not appear to significantly decrease the $(Zn_i)_{Zn}$ signal, no conclusions on this question could be made.

4. Conversion during electron irradiation

The possible importance of conversion processes occurring during the electron irradiation as a result of the accompanying ionization was also explored. To accomplish this, an as-grown PhL sample was first irradiated along a $[\overline{111}]$ direction to produce preferential alignment of the pairs along that direction. It was then annealed to 150 K in the dark, followed by 458 nm excitation at 25 K and a rapid cooldown. At this point, the zinc interstitial was in its $(Zn_i)_{Zn}$ configuration, the *A* and *C* configurations were mostly gone, and the other pairs were still present with their alignments intact. The sample was then electron irradiated in small steps along the opposite, i.e., [111] direction, and the intensity and alignment of the relevant defects were monitored.

Close pair *A* was observed to grow in linearly with dose, but with alignment *opposite* to its initial sense and fully consistent in sense and magnitude with that expected for the [111] beam direction. Since we have established in Sec. III A that the optically induced return of *A* retains its *initial* alignment, we can conclude that during electron irradiation, the $B \rightarrow A$ conversion rate is significantly less than the primary production rate of defect *A*. The $(Zn_i)^+_{Se}$ signal was also observed to grow in, but the growth rate of its fractional concentration was no greater than (roughly equal to) that of the initial interstitial production rate itself. We can conclude, therefore, that contribution of the ionization during the electron irradiation to the rearrangements and separations of the pairs is not significant. This implies that the initial various close and well separated pairs must result from the primary collision event, the recoiling interstitial traveling these various distances before settling down.

Additional important insight comes if we attempt a rough quantitative analysis of the results: Comparing the $(Zn_i)^+_{Se}/[(Zn_i)^+_{Zn}+(Zn_i)^+_{Se}]$ ratio versus electron irradiation dose to that of Fig. 7 versus optical excitation dose suggests a net conversion constant of $\sim 10^{17}$ e/cm^2 for the electron irradiation versus ~ 100 min at 27 mW excitation for the optical excitation. With the sample thickness of 1 mm, approximately 730 keV of electron energy is lost in passing through the sample[13] and, with $3E_g$ per electron-hole pair formed,[14] this gives 8.7×10^4 e-h pairs formed in the crystal per incoming electron. Multiplying this by the sample area

$=1.5\times2.8$ mm^2 and 10^{17} e/cm^2 gives 3×10^{20} e-h pairs produced in the sample for the conversion constant. The failure to detect the ionization component during the electron irradiation suggests that the conversion rate for the ionization alone is, say, $\leqslant 20\%$ of the production rate, giving the *lower limit* of $\gtrsim 1.5\times10^{21}$ e-h pairs required in the volume of the sample for the ionization alone to accomplish $1/e$ of the conversion. On the other hand, the optical excitation of 100 min with 27 mW of 458 nm excitation corresponds to a total of 3×10^{20} photons incident on the sample. An *upper limit*, therefore, to the conversion constant for optical excitation is $\leqslant 3\times10^{20}$ photons, which could occur only if all the light were absorbed in the crystal. This strongly suggests that the photons are more effective than they would be if they simply produced ionization, which is again limited to a maximum of one e-h pair per photon.

This tells us that it is not the ionization accompanying the optical excitation that supplies the dominant mechanism for migration at 1.5 or 4.2 K. Instead, direct optical excitation in the broadband indicated in Fig. 8 must be involved. On the other hand, there is strong evidence that the rapid increase in the process at and above 10 K reflects the increasing effectiveness of ionization with temperature. This comes from early EPR studies, where the production by electron irradiation at 20.4 K produced the closest pairs linearly and isolated zinc vacancies quadratically versus dose.[1] This is fully consistent with the observation presented in Fig. 2 for optical excitation at 25 K, where the closest pairs are relatively more stable but the others are quickly swept apart.

IV. DISCUSSION

A. Zn_i migration mechanism

Previous studies have established that the zinc interstitial is stable in the dark up to ~ 240 K, from which an activation barrier for diffusion of ~ 0.6–0.8 eV could be estimated.[2] We have shown here, however, that *optical excitation at even as low as 1.5 K can cause it to migrate*, and we have established further that the specific motion involved is that of *hopping back and forth between the tetrahedral sites surrounded by four Se atoms and those surrounded by four Zn atoms*. This REM process is temperature independent up to ~ 4.2 K, i.e., *athermal*, but its rate increases rapidly above.

The migration can also be stimulated by electron-hole recombination accompanying the electron-irradiation-produced ionization, as clearly evidenced in the early EPR studies for which the irradiations were performed at 20.4 K.[4] However, we find here that at 4.2 K, the contribution of the enhanced migration processes during the irradiation can be ignored with respect to the initial damage recoil production. This leads to the interesting conclusion, not at all obvious at the outset, that after a 4.2 K irradiation, the distribution of the various Frenkel pairs, from close to distant, is the result of the initial Rutherford scattering event, *the recoiling interstitial traveling the indicated distances before coming to rest*.

Our studies further indicate that at $\leqslant 4.2$ K, optical excitation is more efficient than ionization in producing the interstitial migration, but that in the 10–25 K region where the rate greatly increases, it increases for both processes, with ionization therefore beginning to play an important role in the damage product evolution. Such a strong temperature dependence suggests a carrier capture barrier which requires thermal energy for the carrier to overcome. Evidence of its importance in the optical excitation process as well comes from the dependence of the relative $B \rightleftarrows A$ conversion rates upon the preirradiation history of the sample, not expected if only direct optical excitation is involved, but reflecting instead the existence of competing capture processes.

Another interesting difference exists between the result of elevated temperature annealing in the dark and the low-temperature electronically stimulated processes that we observe here. When annealing in the dark, the close pairs disappear first, with each of the more distant pairs disappearing progressively at higher temperatures according to their separation.[2] When the isolated interstitials finally disappear, no evidence of the normally stable isolated vacancies remains. As pointed out in this earlier study, this supplies strong evidence of inward collapse and annihilation of the pairs, as the migrating positive interstitial is drawn toward the negative vacancy, as expected. The result we find for the optically induced interstitial migration here is the reverse. The closest pairs are the most stable and the interstitial clearly migrates away from the vacancy.

This suggests that during the REM process, the strong Coulomb attraction is absent, which is best explained if the interstitial is in its neutral, or even possibly negative, charge state. (The zinc vacancy is not believed to possess a neutral state in the gap.[2]) Before pursuing the consequences of this idea further, however, let us first consider two other pieces of evidence that may be related. (i) Consider the fact that the migration jump has been established to be from one tetrahedral site to another. This is a surprise because, in either T_d site, only breathing (A_1) vibrational modes are expected to be stimulated by changes between charge states $++$, $+$, and 0, the ground states all expected to be S states (A_1). Such modes supply no off-center ''kick'' in the diffusive direction upon electron or hole capture. There could be substantial breathing mode relaxational changes, but in the notation of Stoneham, the ''accepting'' and ''promoting'' modes are orthogonal.[8] If, however, electron capture is into an excited p-orbital (T_2), which, in turn, goes deep as it undergoes a trigonal (T_2) Jahn-Teller distortion, the interstitial atom could get the appropriate ''kick.'' A well studied example of this is the double donor As_{Ga} antisite in GaAs (the $EL2$ center), whose off-center metastable configuration for its *neutral* state has been described in this manner.[15] Alternatively, of course, there could be a deep off-center configuration associated with a *negative* charge state for the defect, similar to the DX phenomenon, where the large lattice relaxational energy gain of its normal p state overcomes the Coulomb electron-electron repulsion and provides the deep binding for the extra electron. (ii) In no spectral region is the ODEPR spectrum of either interstitial positive, suggesting that the donor to $(Zn_i)^+$ recombination of Eq. (2) is either nonradiative or at least Stokes-shifted out of our detector range.

These three observations all appear consistent with the idea that the motion is stimulated by electron capture by $(Zn_i)^+$ into an excited state of $(Zn_i)^0$, which Jahn-Teller distorts, giving the interstitial atom an appropriate ''kick'' toward the other site in its *neutral* charge state, and diverting

a substantial part of the recombination energy from luminescence to the kinetic energy of the atoms as they are propelled to their new equilibrium configuration. Modern state-of-the-art local-density calculations have displayed remarkable success in the DX and $EL2$ problems,[16,17] and it would be highly desirable for similar calculations to be performed for interstitial zinc in ZnSe to test this idea.

B. $(Zn_i)_{Zn} \rightarrow (Zn_i)_{Se}$ conversion in the dark

The detailed mechanism responsible for the $(Zn_i)_{Zn} \rightarrow (Zn_i)_{Se}$ conversion in the dark at 25 K is not clear. It cannot be simple thermally activated motion over a small barrier because in material which has accumulated several previous irradiations, only partial conversion occurs and it is necessary to anneal to ~ 150 K before it is complete. In the n-type material, it is not apparent that it occurs at all. Also, in the as-grown samples, it has sometimes been noted that annealing at ~ 70 K in the dark actually serves to generate some $(Zn_i)^+_{Zn}$, where there was none before, with its disappearance upon subsequent anneal at ~ 90 K. We are tempted to conclude, therefore, that the processes somehow reflect capture of carriers that are being released at these low temperatures, the capture being less efficient in competition with defects accumulated from the previous irradiations, and their effect upon the charge occupancies of other defects, etc. The logical choice for the 25 K anneal is the release of electrons trapped at the shallow donors after optical excitation, which, at $\sim E_C - 0.027$ eV,[18] should be occurring in this temperature region. This could be consistent with the apparent lack of the effect in n-type material if there the intertstitials were already in their neutral state before the anneal.

C. Assignment of Frenkel pair separations

In the optically induced regeneration of close pair A, Fig. 3, it reemerges with alignment memory of the original damage event. The observation that its alignment matches closely that of B, from which it is being regenerated, is, of course, reasonable. At the same time, however, it may also supply further valuable information concerning the proper choice of the assignments for the interstitial positions of each. The observed symmetry and alignment properties of B have previously been interpreted to identify it as arising from a pair with the interstitial displaced in a $\langle 100 \rangle$ direction from the vacancy.[2] The A site, in turn, should therefore reasonably be chosen as a $(Zn_i)_{Se}$ site to which a single $(Zn_i)_{Se} \rightarrow (Zn_i)_{Zn} \rightarrow (Zn_i)_{Se}$ diffusional jump step can carry it. The particular choice made for A in Ref. 3 does not appear to satisfy this, and, factoring in this new information, a better choice could be made. For example, taking the $(300)a/2$ interstitial to vacancy distance assignment for B made there, a better choice for A might be the previously unassigned $(210)a/2$ pair (see Table I in Ref. 3). Alternatively, the possibility that B arises from the closer unassigned $(100)a/2$ pair may also have to be reconsidered, with corresponding changes for A. We will not attempt these reassignments here, except to note that a detailed study of the intraconversions between the various pairs, such as that of $A \rightleftarrows B$ studied here, can potentially supply critical additional information concerning the proper lattice assignments for the pairs. Such studies in the future would be valuable in this regard.

D. Electronic structure of $(Zn_i)^+$ in the two sites

Let us now consider what has been learned about the properties of isolated $(Zn_i)^+_{Zn}$. Its increased central hyperfine interaction and the more rapid dropoff versus distance for its neighboring Se atom hyperfine interactions compared to $(Zn_i)^+_{Se}$ clearly indicate that its electron is more tightly bound, and correspondingly, its second donor level $(+/++)$ is deeper. This result has already been incorporated schematically in Fig. 1. From the slope of the radial dropoff (Fig. 6), the $(+/++)$ second donor level positions were estimated to be at $\sim E_C - 1.2$ eV for $(Zn_i)_{Se}$ and $\sim E_C - 1.8$ eV for $(Zn_i)_{Zn}$. Strictly speaking, the slopes should reliably reflect the level positions only for the tail of the envelope wave function, well removed from the core, so our estimates here can actually serve only as approximate guides. Still, it is interesting to compare these to the recent state-of-the-art *ab initio* local-density theoretical calculations for the zinc interstitial.[11,12] There, the second donor levels were estimated to be at $E_V + 1.47$ eV and $E_V + 1.03$ eV, for $(Zn_i)_{Se}$ and $(Zn_i)_{Zn}$, respectively. With the band-gap of 2.82 eV, these would correspond to $E_C - 1.35$ eV and $E_C - 1.79$ eV, in remarkable agreement with the estimates deduced here from the wave-function dropoff.

However, this apparent detailed agreement must be considered to a large degree accidental, because such local-density calculations also inevitably contain substantial uncertainties when estimating level positions in the band gap. For example, the band gap in the calculations was actually only ~ 1 eV. Therefore, since both theory and our simple estimates from the experimental radial dropoff of the wave functions near the core contain substantial uncertainties, the indicated positions of the levels in the band gap must be considered similarly uncertain. For example, an alternative experimental estimate of $E_C - 0.9$ eV was also made for the $(Zn_i)_{Se}$ $(+/++)$ level in the earlier work by considering the photoluminescence energy of one of the Frenkel pairs (X_8) whose separation was believed to be established as the $(500)a/2$pair.[2] Assuming a proportional experimental overestimate here for $(Zn_i)^+_{Zn}$ suggests its level to be $\sim$0.4-0.5 eV lower, i.e., at $\sim E_C - 1.4$ eV. Alternatively, if a reassignment of B to the $(100)a/2$ pair is a possibility, as suggested above, this would open up the closer $(300)a/2$ site for X_8. In this position, the increased Coulomb interaction between the pair would lead to an estimate of $E_C - 1.1$ eV for the $(Zn_i)_{Se}$ $(+/++)$ level, now close again to our estimate from the dropoff of the hyperfine interactions. Considering these uncertainties, we tentatively place the $(+/++)$ levels at $E_C - 1.0$ eV for $(Zn_i)_{Se}$ and $E_C - 1.6$ eV for $(Zn_i)_{Zn}$, but with approximate error bars of ± 0.3 eV. The differences in the theoretically predicted energy-level positions, ~ 0.45 eV, can be expected to cancel some of the theoretical uncertainties, and its reasonable agreement with the experimental estimates is correspondingly more significant.

The as yet unsuccessful search for ODEPR signals from Frenkel pairs involving $(Zn_i)_{Zn}$ was motivated by the attempt to establish more directly the difference in level positions for the two interstitials. As can be seen in Fig. 1, the PL energy for each of the $(Zn_i)_{Zn}$ Frenkel pairs should be lower in energy than that for the corresponding $(Zn_i)_{Se}$ pair by approximately the energy difference between the isolated interstitial $(+/++)$ levels. Discounting the closer pairs which show in Fig. 10 little evidence for effective conversion to the $(Zn_i)_{Zn}$ pairs, the PL of X_8 and the progressively more distant pairs, which do display evidence of increasingly effective conversion, peaks at $\leqslant 1.2$ eV.[2] An energy difference of 0.5 eV already shifts the PL for the corresponding $(Zn_i)_{Zn}$ pairs to $\leqslant 0.7$ eV ($\geqslant 1.77$ μm), which is just beyond the cutoff of the Ge detector. The failure to detect the signals appears therefore fully consistent with our estimate that the isolated $(Zn_i)_{Zn}$ $(+/++)$ level is $\gtrsim 0.5$ eV deeper than that for $(Zn_i)_{Se}$.

Attempts to detect positive ODEPR signals for either of the isolated interstitials were also unsuccessful. We know that recombination is occurring between the shallow donor and the first donor $(0/+)$ level of each of the isolated interstitials, as indicated in Fig. 1 and Eq. (2), because we detect the process by negative ODEPR signals as it competes with PL from other sources throughout the full spectral range. If the processes were efficiently radiative, and in our spectral range, we should have detected them as positive signals and their spectral positions could have supplied a direct measurement of the corresponding $(0/+)$ single donor level. The failure to detect them implies that one or the other of these two conditions is not met. We have no direct or indirect experimental information on the single $(0/+)$ donor level positions, and the transitions would not have been detected if their levels were $\lesssim 0.7$ eV below the conduction band, being again outside of our Ge detector range. This is of course possible, the first donor state of a double donor often being less than half as deep as its second donor state. However, theoretical estimates have also been made by Laks *et al.*,[11,12] which place the $(0/+)$ levels at $E_V+1.68$ eV and $E_V+1.27$ eV for $(Zn_i)_{Se}$ and $(Zn_i)_{Zn}$, respectively, which, with $E_g=2.82$ eV, gives $E_C-1.14$ eV and $E_C-1.55$ eV. If they are in fact this deep, we certainly should have seen them if they are radiative. The model discussed earlier, that the process is nonradiative, or at least Stokes-shifted out of our spectral range, remains an attractive alternative explanation. In that case, the electron could be transfering to an excited *p* state of the neutral interstitial, with a substantial part of the recombination going into Jahn-Teller distortion, which gives it the necessary ''kick'' for the diffusion jump.

Theoretical estimates of the hyperfine interactions have also been made for both $(Zn_i)^+_{Zn}$ and $(Zn_i)^+_{Se}$,[19,20] and compared to the experimental values in Table I. As already pointed out by these authors, their theoretical estimates for the central zinc and neighboring Se neighboring shells of $(Zn_i)^+_{Se}$ agree closely with the previously observed experimental values. In the case of $(Zn_i)_{Zn}$, their values were predicted in advance of our present studies, and are also in good agreement with our results. We must conclude that such *ab initio* local-density calculations can be remarkably accurate, at least as evidenced here for the (Zn_i) charge states.

V. SUMMARY

We have established the following.

(i) Migration of interstitial zinc in ZnSe can be caused by optical excitation at 1.5 K into a broadband below the band gap. The rate is independent of temperature up to 4.2 K but increases rapidly by 10 K and higher.

(ii) Its migration occurs by hopping between the T_d interstitial site surrounded by four Se atoms, $(Zn_i)_{Se}$, and that surrounded by four zinc atoms, $(Zn_i)_{Zn}$.

(iii) Its migration can also be stimulated by electron-hole pair recombination resulting from the ionization produced during the electron-irradiation. At 4.2 K, its effect is negligible with respect to the Frenkel pair production rate. The many distinct pairs of different separations present after 2.5 MeV electron irradiation at 4.2 K are therefore the result of the initial Rutherford scattering event. During irradiation at 20.4 K, however, the process becomes comparable to that of pair production.

(iv) Its optically induced migration causes separation of the pairs, in contrast to pair annihilation under elevated temperature annealing in the dark, suggesting it migrates in its neutral (or negative) charge state.

(v) In freshly irradiated as-grown crystals, annealing in the dark at 25 K causes near-complete $(Zn_i)_{Zn} \rightarrow (Zn_i)_{Se}$ conversion. This is not true for repeatedly reirradiated samples or for low resistivity *n*-type samples, revealing that the process is probably associated with a charge-capture process, and not evidence of a very low energy barrier between the two configurations.

(vi) ODEPR has been detected for $(Zn_i)^+_{Zn}$, and hyperfine interactions for the central ^{67}Zn its six next-nearest ^{77}Se neighbors are determined. From these, a rough estimate of its second donor level $(+/++)$ position has been made, indicating $\sim E_C-1.8$ eV, compared to a corresponding estimate of $\sim E_C-1.2$ eV for $(Zn_i)_{Se}$. Factoring in other considerations, the $(+/++)$ level positions have been placed tentatively at $E_C-1.6$ eV for $(Zn_i)_{Zn}$ and $E_C-1.0$ eV for $(Zn_i)_{Se}$, with approximate error bars of ± 0.3 eV.

(vii) No luminescence has been detected that could be associated directly with (i) close pairs involving $(Zn_i)^+_{Zn}$, or (ii) the $(Zn_i)^+ + \mathcal{D}^0 \rightarrow (Zn_i)^0 + \mathcal{D}^+$ recombination process for either isolated interstitial configuration. The $(Zn_i)^+_{Zn}$ close pair luminescence likely occurs at too long a wavelength for our detection. That could also be the case for the isolated $(Zn_i)^+ + \mathcal{D}^0$ recombination, but an alternative explanation is that the process is nonradiative, or Stokes-shifted out of the range of our detectors, the energy being utilized for the migration process. A model has been suggested for such a process in which electron capture into the neutral state occurs via an excited *p* state, which trigonally Jahn-Teller distorts, providing the necessary ''kick'' for conversion between the two sites. This would be consistent with conclusions (iv) and (v) above.

(viii) The electron-irradiation produced PL band with ZPL at 0.907 eV is presumably intrinsic-defect related but is not in any way related to the zinc interstitial, as had been previously suggested. Hence, an interesting possibility is that this signal is due to an intrinsic defect on the Se sublattice.

(ix) Our results for the level positions and hyperfine interactions of the two interstitial configurations agree remark-

ably with recent theoretical results for these quantities. This can be interpreted to provide a strong and perhaps unique confirmation of the reliability of such *ab initio* local-density calculations for interstitial defects. With this apparent success, it is hoped that this will stimulate these authors, and possibly others, to probe the various diffusion mechanisms that have been proposed here.

ACKNOWLEDGMENTS

Many helpful discussions with M. Stavola are gratefully acknowledged. This research was supported by National Science Foundation Grants Nos. DMR-92-04114 and DMR-97-04386, and, in its initial stages, by the Office of Naval Research, Electronic Division, Grant No. N00014-94-0117.

[1] G.D. Watkins, Phys. Rev. Lett. **33**, 223 (1974).
[2] F.C. Rong, W.A. Barry, J.F. Donegan, and G.D. Watkins, Phys. Rev. B **54**, 7779 (1996).
[3] W.A. Barry and G.D. Watkins, Phys. Rev. B **54**, 7789 (1996).
[4] F. Rong and G.D. Watkins, Phys. Rev. Lett. **58**, 1486 (1987).
[5] K.H. Chow and G.D. Watkins, Phys. Rev. Lett. **81**, 2084 (1998).
[6] L.C. Kimerling, Solid-State Electron. **21**, 1391 (1978).
[7] J.C. Bourgoin and J.W. Corbett, Radiat. Eff. **36**, 157 (1978).
[8] A.M. Stoneham, Rep. Prog. Phys. **44**, 1251 (1981).
[9] Since the hyperfine interaction is axially symmetric about a $\langle 100 \rangle$ axis, $A_{\rm eff} = \sqrt{A_{\parallel}^2 \cos^2\theta + A_{\perp}^2 \sin^2\theta}$, where θ is the angle between the **B** and the $\langle 100 \rangle$ direction.
[10] E. Clementi and C. Roetti, At. Data Nucl. Data Tables **14**, 177 (1974).
[11] D.B. Laks, C.G. Van de Walle, G.F. Neumark, P.E. Blöchl, and S.T. Pantelides, Phys. Rev. B **45**, 10 965 (1992).
[12] The values indicated for the interstitial level positions were not specifically given in Ref. 11, but derive from that work. They were supplied to us privately by C.G. Van de Walle.
[13] J.W. Corbett, in *Electron Radiation Damage in Semiconductors and Metals*, Supplement 7 of *Solid State Physics*, edited by H. Ehrenreich, F. Seitz, and D. Turnbull (Academic Press, New York, 1966), p. 35.
[14] C.A. Klein, J. Appl. Phys. **39**, 2029 (1968).
[15] G. D. Watkins, Semicond. Sci. Technol. **6**, B111 (1991).
[16] D. J. Chadi and K. J. Chang, Phys. Rev. Lett. **60**, 2187 (1988); Phys. Rev. B **39**, 10 063 (1989).
[17] J. Dabrowski and M. Scheffler, Phys. Rev. Lett. **60**, 2183 (1988); Phys. Rev. B **40**, 10 391 (1989).
[18] J.L. Mertz, H. Kukimoto, K. Nassau, and J.W. Schiever, Phys. Rev. B **6**, 545 (1972).
[19] C. G. Van de Walle and P.E. Blöchl, Phys. Rev. B **47**, 4244 (1993).
[20] A. Illgner and H. Overhof, Phys. Rev. B **54**, 2505 (1996).